

Characterization of hydrogen etched 6H-SiC(0001) substrates and subsequently grown AlN films

Cite as: Journal of Vacuum Science & Technology A 21, 394 (2003); <https://doi.org/10.1116/1.1539080>
Submitted: 11 July 2002 • Accepted: 18 November 2002 • Published Online: 05 February 2003

J. D. Hartman, A. M. Roskowski, Z. J. Reitmeier, et al.



View Online



Export Citation

ARTICLES YOU MAY BE INTERESTED IN

[Step control of vicinal 6H-SiC\(0001\) surface by \$H_2\$ etching](#)

Journal of Applied Physics **97**, 104919 (2005); <https://doi.org/10.1063/1.1901838>

[Mechanisms of growth and defect properties of epitaxial SiC](#)

Applied Physics Reviews **1**, 031301 (2014); <https://doi.org/10.1063/1.4890974>

[Precise in situ thickness analysis of epitaxial graphene layers on SiC\(0001\) using low-energy electron diffraction and angle resolved ultraviolet photoelectron spectroscopy](#)

Applied Physics Letters **93**, 033106 (2008); <https://doi.org/10.1063/1.2960341>



Advance your science and
career as a member of

AVS

LEARN MORE



Characterization of hydrogen etched 6H-SiC(0001) substrates and subsequently grown AlN films

J. D. Hartman,^{a)} A. M. Roskowski, Z. J. Reitmeier, K. M. Tracy, and R. F. Davis
Materials Science and Engineering, North Carolina State University, Raleigh, North Carolina 27695

R. J. Nemanich
Department of Physics, North Carolina State University, Raleigh, North Carolina 27695

(Received 11 July 2002; accepted 18 November 2002; published 5 February 2003)

Wafers of *n*-type, 6H-SiC(0001) with $(N_D - N_A) = (5.1 - 7.5) \times 10^{17}$ and 2.5×10^{18} were etched in a flowing 25% H₂/75% He mixture within the range of 1500–1640 °C at 1 atm. Equilibrium thermodynamic calculations indicated that the presence of atomic hydrogen is necessary to achieve etching of SiC. Atomic force microscopy, optical microscopy, and low energy electron diffraction of the etched surface revealed a faceted surface morphology with unit cell and half unit cell high steps and a 1×1 reconstruction. The latter sample also exhibited a much larger number of hexagonal pits on the surface. Annealing the etched samples under ultrahigh vacuum (UHV) at 1030 °C for 15 min resulted in (1) a reduction of the surface oxygen and adventitious hydrocarbons below the detection limit of Auger electron spectroscopy, (2) a $(\sqrt{3} \times \sqrt{3})R30^\circ$ reconstructed surface and (3) a Si-to-C peak-to-peak height ratio of 1.2. By contrast, using a chemical vapor cleaning (CVC) process consisting of an exposure to 3000 Langmuir (L) of silane at 1030 °C for 10 min under UHV conditions resulted in a (3×3) surface reconstruction, a Si-to-C ratio of 3.9, and islands of excess silicon. Continued annealing of the latter material for an additional 10 min at 1030 °C resulted in a (1×1) LEED pattern with a diffuse ring. Films of AlN grown via MOCVD at a sample platter temperature of 1274 °C for 15 min on hydrogen etched wafers having a doping concentration of $8.7 \times 10^{17} \text{ cm}^{-3}$ and cleaned via annealing had a rms roughness value of $\approx 0.4 \text{ nm}$. © 2003 American Vacuum Society. [DOI: 10.1116/1.1539080]

I. INTRODUCTION

Aluminum nitride (AlN) with a room temperature band gap of 6.2 eV has realized and potential applications, both as a substrate and as a component in thin film solutions with other III nitrides, in high-power, high-frequency, and high-temperature microelectronic devices as well as optoelectronic devices that operate in the ultraviolet portion of the spectrum. The lack of readily available bulk single crystals of this material for the former application requires that it be grown heteroepitaxially on substrates such as sapphire or 6H-SiC. The (0001) surfaces of as-polished wafers of the latter substrate contain steps that are one Si/C bilayer in height. As such, there is a mismatch between these steps and the double bilayer stacking sequence of the wurtzite AlN along [0001]. This results in the formation of stacking mismatch boundaries in the AlN.^{1,2} One method to reduce the density of these defects is to produce steps on the surfaces of the 6H-SiC(0001) substrates, with heights equal to an integer multiple of the unit cell height of AlN, via etching of the surface in hydrogen at $\sim 1600^\circ\text{C}$.²

Etching of 4H(0001) and 6H-SiC(0001) surfaces in flowing hydrogen results in unit cell height steps of 1.0 and 1.5 nm, respectively. These steps form as either periodic arrays^{3,4} or hexagonal patterns, with the latter a result of the intersection of screw dislocations with the surface.⁴ The chemical and structural analysis of the (0001) surface of 6H-SiC and

of the (0001) surface of 4H-SiC wafers after exposure to flowing hydrogen at 1500 °C for 5 min have revealed a $(\sqrt{3} \times \sqrt{3})R30^\circ$ LEED pattern as a result of a highly ordered monolayer of silicon oxide.⁵ Investigations regarding the *in situ* surface preparation of the etched surface have focused on thermal annealing⁵ and the deposition of silicon followed by flash evaporation of this element at elevated temperatures.⁶

In the present research, the microstructures of hydrogen etched 6H-SiC(0001) surfaces have been investigated with respect to the net ionized carrier concentrations of the silicon carbide substrates. The etched surfaces were then exposed to an *in situ* chemical vapor clean using silane and the resulting surface chemistry compared to that obtained by thermal annealing. Films of AlN were subsequently grown via MOVPE on both the hydrogen etched and the unetched surfaces and characterized using atomic force microscopy (AFM).

II. EXPERIMENTAL PROCEDURES

Diced 10 mm \times 10 mm samples from on-axis, *n*-type 6H-SiC(0001) wafers were chemically cleaned in boiling trichloroethylene, acetone, and methanol for 10 min in each solvent; dipped into a 10:1 HF acid solution for 10 min to remove 50–100 nm of thermally grown silicon oxide; rinsed in deionized water for at least 10 s; and dried in flowing

^{a)}Electronic mail: jhartmanchartman@aol.com

TABLE I. Summary of samples and the environment to which they were exposed. Sample H was etched at Carnegie Mellon at 1600 to 1700 °C for 15 min at 1 atm with 14 lpm of hydrogen.

Sample	$N_D - N_A$ (cm^{-3})	Etched in H_2	Thermally annealed	CV clean w/ SiH_4	CV clean w/ SiH_4 + anneal	MOCVD AlN
A	$7.5 \times 10^{17\dagger}$	X				
B	2.5×10^{18}	X				
C	5.1×10^{17}	X	X			
D	5.1×10^{17}	X		X		
E	5.1×10^{17}	X			X	
F	n/a		X			X
G	$8.7 \times 10^{17\dagger}$	X	X			X
H	2.8×10^{18}	X	X			X

[†]Value measured on a similar sample from the same wafer.

nitrogen. The samples were subsequently used for studies involving either hydrogen etching or AlN deposition, as summarized in Table I.

For the etching research, the samples were immediately mounted onto a 12 mm wide by 75 mm long Ta strip heater, enclosed within a water-cooled quartz chamber that was evacuated to a base pressure <100 mTorr, and heated to the desired temperature in 1 slm of a 25% hydrogen/75% helium mixture. All samples were etched using an 8 slm flow rate of this mixture, a period of 20 min, and a pressure of 1 atm. Optimal etching temperature ranges for samples having net ionized carrier concentrations of $(3-7) \times 10^{17} \text{ cm}^{-3}$ and $>2 \times 10^{18} \text{ cm}^{-3}$ were achieved at 1600–1630 and 1490–1520 °C, respectively. The reason(s) for the different optimum conditions is not known at this time. The temperature of the silicon carbide wafer was monitored using an optical pyrometer with an emissivity setting of 1.0. The samples were rapidly cooled while maintaining the 8 slm flow rate and the 1 atm pressure, characterized via optical microscopy (OM) and AFM and subsequently used for either *in situ* cleaning studies or growth of AlN films. A Nomarski interference filter was employed with the optical microscope.

In preparation for the cleaning studies, tungsten was deposited via rf sputtering on the carbon face of each 6H-SiC wafer to maximize the absorption of radiation during heating. Each wafer was again exposed to the above solvent clean followed by a 10 min exposure to the vapor from a 30:1 HF buffered oxide etching solution. The efficacy of the two cleaning processes was investigated. Samples cleaned via thermal desorption were ramped to a surface temperature of 1030 °C, as measured by an optical pyrometer with an emissivity setting of 0.5, and held for 15 min at $\approx 1 \times 10^{-8}$ Torr. Characterization was conducted on each cleaned sample using Auger electron spectroscopy (AES), low energy electron diffraction (LEED), x-ray photoemission spectroscopy (XPS), and AFM.

The chemical vapor cleaning (CVC) process involved the exposure of selected samples to silane in a molecular beam epitaxy chamber having a base pressure of 9×10^{-10} Torr. The samples were ramped at 30°/min to 960 °C at which time a collimated, focused beam of silane was introduced

into the system. Each sample was then ramped to 1030 °C, held for 10 min, resulting in an exposure of 3000 L of silane, and cooled at 40 °C/min under flowing silane to 650 °C to maintain the (3×3) reconstruction obtained as a result of the cleaning. As a check on the short term stability of this reconstruction, selected samples, previously exposed to the CV cleaning, were annealed in the MBE chamber at 5×10^{-9} Torr for an additional 10 min at 1030 °C. Characterization techniques similar to that used in the thermal desorption studies were also employed in this component of the research.

During a single growth run, aluminum nitride films were deposited via MOCVD on (1) a sample having a net ionized carrier concentration of $8.7 \times 10^{17} \text{ cm}^{-3}$ and etched using the above mentioned hydrogen/helium mixture and the associated conditions; (2) a sample having a net ionized carrier concentration $2.8 \times 10^{18} \text{ cm}^{-3}$ and previously etched in pure hydrogen at Carnegie Mellon University,⁴ and (3) an unetched sample. Prior to growth, the samples were annealed at ~ 1275 °C for 15 min in hydrogen flowing at 3 slm to evaporate residual oxide from the surface. The AlN films were grown at a total pressure and sample platter temperature of 20 Torr and ~ 1275 °C (emissivity=0.8), respectively, for 30 min in a water-cooled vertical pancake-style quartz chamber using trimethylaluminum and ammonia as the reactants. The resulting samples were characterized using atomic force and optical microscopies.

III. RESULTS AND DISCUSSION

A. Thermodynamic considerations

Etching of silicon carbide in flowing hydrogen has been suggested to occur via the evaporation of silicon and the formation of hydrocarbons.^{7,8} Kumagawa *et al.*⁸ proposed that the SiC surface dissociates into liquid silicon and solid carbon followed by the vaporization of the former. Hallin *et al.*⁹ also suggested that liquid silicon droplets would form if silicon carbide were allowed to freely decompose in flowing hydrogen within the temperature range of 1400–1600 °C. This latter group further proposed that the addition of hydrocarbons to the hydrogen could reduce the etching rate and therefore suppress the formation of silicon droplets. Proof of the above mentioned suggestions has been presented by Burk *et al.*¹⁰ who observed the formation of silicon droplets on 6H- and 4H-SiC(0001) wafers in the temperature range of 1450–1520 °C but did not observe the droplets when hydrocarbons were present in the chamber in the same temperature range.

Initial analyses by Chu *et al.*⁷ and Kumagawa *et al.*⁸ showed that the calculated free energy of formation for acetylene and methane at 1727 °C are +28 and +31 kcal/mol, respectively. Table II shows the values for the free energy of formation/mole for these hydrocarbons calculated in the present research from 1400 to 1700 °C in 100 °C increments using HSC Chemistry software.¹¹ The values were in good agreement with prior results, especially at the higher temperatures. Also shown in Table II are the free energies of dissociation of SiC, the evaporation of silicon, the formation

TABLE II. Free energies of formation/reaction for potential reactions during the hydrogen etching of 6H-SiC(0001) surfaces. Values of ΔG were calculated using HSC Chemistry data and application (see Ref. 11).

Reaction	ΔG_i (kcal/mol)			
	1400 °C	1500 °C	1600 °C	1700 °C
SiC=Si+C	14.6	13.8	12.9	12.0
H ₂ (g)=2H	60.4	57.5	54.7	51.8
Si=Si(g)	48.8	46.0	43.3	40.6
2C+H ₂ =C ₂ H ₂	32.1	30.8	29.6	28.3
0.5C+H ₂ =0.5CH ₄	11.3	12.6	13.9	15.3
0.5Si+H ₂ =0.5SiH ₄	22.5	24.0	25.6	27.1
1/2SiC+H ₂ =1/2Si+1/2CH ₄	18.5	19.5	20.4	21.3
2SiC+H ₂ =2Si+C ₂ H ₂	61.2	58.4	55.4	52.4
1/4SiC+H ₂ =1/4SiH ₄ +1/4CH ₄	20.5	21.8	23.0	24.2
2/5SiC+H ₂ =2/5SiH ₄ +1/5C ₂ H ₂	30.3	30.9	31.5	32.1
C+H=1/2C ₂ H ₂	-14.2	-13.4	-12.5	-11.7
1/4C+H=1/4CH ₄	-24.6	-22.5	-20.4	-18.3
1/4Si+H=1/4SiH ₄	-18.9	-16.7	-14.6	-12.4
1/4SiC+H=1/4Si+1/4CH ₄	-20.9	-19.0	-17.1	-15.3
SiC+H=Si+1/2C ₂ H ₂	0.4	0.4	0.4	0.3
1/5SiC+H=1/5SiH ₄ +1/10C ₂ H ₂	-15.0	-13.3	-11.6	-9.8
1/8SiC+H=1/8SiH ₄ +1/8CH ₄	-19.9	-17.9	-15.8	-13.8

of silane, and four suggested reactions used to describe the decomposition of silicon carbide in the presence of molecular hydrogen calculated using the same software. All of the reactions in the last set of data show a positive value for the free energy of reaction when calculated using one mole of molecular hydrogen. Thus, none of these reactions would occur spontaneously at these temperatures.

Investigations by Siebert *et al.*¹² showed that the SiC(0001) surface may be terminated by atomic hydrogen in a C₃Si-H configuration that formed as a result of the decomposition of molecular hydrogen on this surface at temperatures as low as a 1000 °C. The etching process at 1600 °C may also be initiated by a similar mechanism, namely, the enhanced dissociation of molecular hydrogen to atomic hydrogen on the Si-terminated SiC surface. The etching would be accomplished by the subsequent reaction of the atomic hydrogen with the silicon and/or the carbon from the dissociation of the SiC to form SiH₄ and/or hydrocarbons. The free silicon may also be removed via direct evaporation. This hypothesis is supported by the thermodynamic data in that the free energies of formation and of reaction wherein SiH₄ and/or the hydrocarbons are products become negative when the reactions are considered to occur in an environment containing atomic hydrogen, as shown in the chemical equations in Table II. The most negative value of ΔG per mole of atomic hydrogen for the reaction of H with SiC occurs when methane and free silicon are the reaction products. The free energy to form silane via reaction of Si with atomic H is increasingly negative as the temperature is decreased. However, within the lower temperature range of 1400–1500 °C it is possible that silicon may remain on the surface in the form of droplets, due to the decreased concentration of atomic hydrogen and/or the slower kinetics of reaction with the H

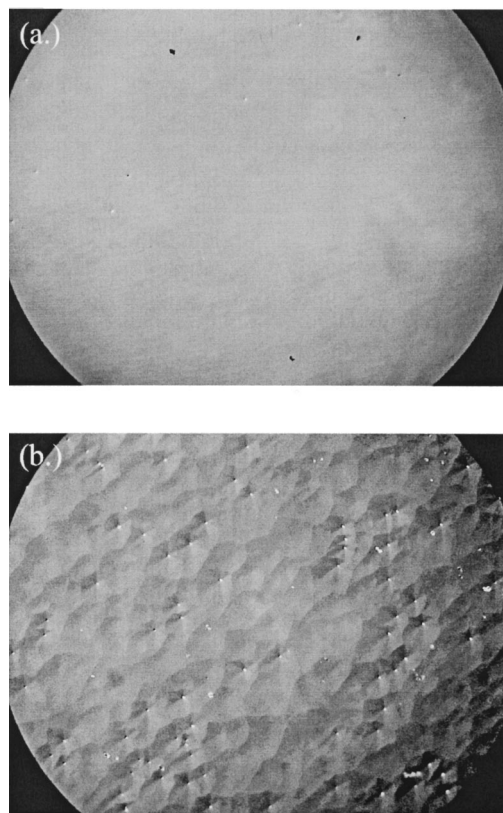


Fig. 1. Optical micrographs obtained at 200 \times using a Nomarski filter of surfaces of hydrogen etched 6H-SiC(0001) with (N_D-N_A) values of (a) $7.5 \times 10^{17} \text{ cm}^{-3}$ and (b) $2.5 \times 10^{18} \text{ cm}^{-3}$.

and/or its lower equilibrium partial pressure at these temperatures.

Sagar *et al.*¹³ observed that the etch rates of on-axis and vicinal 6H-SiC(0001) and 4H-SiC(0001) at temperatures of 1680 and 1720 °C were within a factor of two and not determined by the step and kink densities. They surmised that the etch rate was limited by the concentration of hydrogen atoms. Previous investigations by Harris *et al.*¹⁴ found the etch rate of SiC to be dependent upon the susceptor material which supports the formation of atomic hydrogen due to the different catalytic properties of the different materials. Also, Nakamura *et al.*¹⁵ showed that stepped surfaces may be obtained on SiC(0001) at temperatures around 1300 °C when using HCl/H₂ mixtures, indicating the necessity of atomic hydrogen for this process.

B. Surface preparation

Optical and atomic force micrographs of the surface morphologies of hydrogen etched samples with (N_D-N_A) (and rms roughness) values of $7.5 \times 10^{17} \text{ cm}^{-3}$ (0.51 nm) and $2.5 \times 10^{18} \text{ cm}^{-3}$ (1.32 nm) are shown in Figs. 1(a), 1(b), 2(a), and 2(b), respectively. The former two micrographs show that increasing concentrations of nitrogen and, consequently, net carrier concentrations resulted in an increase in the density of hexagonal etch pits, as also observed by Okamoto *et al.*¹⁶ on similarly derived modified Lely (seeded) 6H-SiC wafers. The AFM image in Fig. 2(a) of the etched

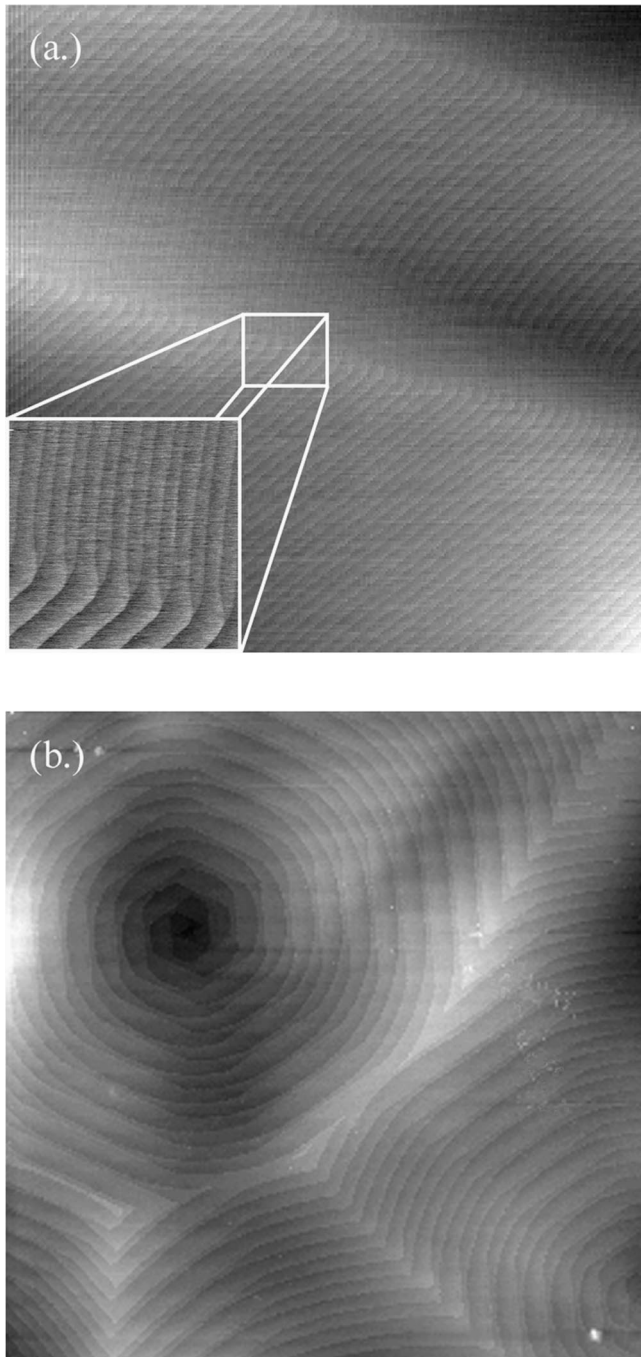


FIG. 2. (a) $30\ \mu\text{m} \times 30\ \mu\text{m}$ AFM image of a hydrogen etched surface of a 6H-SiC(0001) wafer with a $(N_D - N_A) = 7.5 \times 10^{17}\ \text{cm}^{-3}$ showing a change in step structure due to a faulted region in the 6H-SiC(0001). The inset shows a $5\ \mu\text{m} \times 5\ \mu\text{m}$ image of the transition region. (b) Typical hydrogen etched surface of a 6H-SiC(0001) wafer $(N_D - N_A) = 2.5 \times 10^{18}\ \text{cm}^{-3}$.

surface of the sample with $(N_D - N_A) = 7.5 \times 10^{17}\ \text{cm}^{-3}$ shows two distinct regions having step heights of $\sim 1.5\ \text{nm}$ (unit cell height) with a terrace width of $0.7\ \mu\text{m}$ and steps heights of $0.7\ \text{nm}$ ($\sim 1/2$ unit cell height) with a terrace widths of $0.3\ \mu\text{m}$. The height of the steps in the latter region also corresponds to the height of a unit cell of the cubic, 3C-SiC polytype. The AFM image in Fig. 2(b) of the higher doped sample shows major and minor portions of four inter-

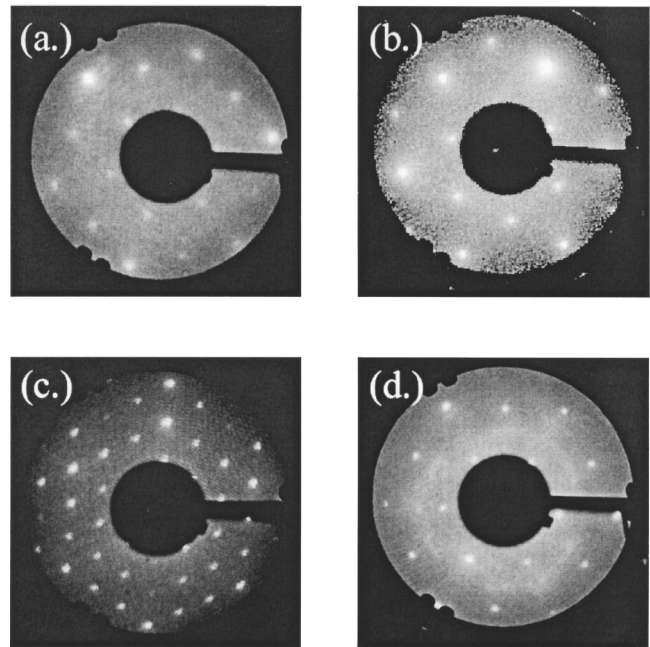


FIG. 3. Representative LEED patterns from 6H-SiC(0001) wafers showing (a) 1×1 pattern from the as-loaded hydrogen etched surface (b) a $(\sqrt{3} \times \sqrt{3})R30^\circ$ pattern of a surface thermally annealed at $1030\ ^\circ\text{C}$ for 15 min, (c) a (3×3) pattern from a surface chemically vapor cleaned in 3000 L SiH_4 at $1030\ ^\circ\text{C}$ for 10 min and (d) 1×1 pattern from a CVC cleaned surface followed by an anneal at $1030\ ^\circ\text{C}$ for 10 min.

secting hexagonal pits produced by the etching of screw dislocations that intersected the surface.⁴ These pits dominated the surface microstructure of this sample; they were not commonly observed in the lower doped wafer, as seen in Fig. 1(a).

The surfaces of as-loaded, hydrogen-etched samples exhibited at (1×1) LEED pattern, regardless of the value of $(N_D - N_A)$, as shown in Fig. 3(a). In comparison, Bernhardt *et al.*⁵ observed $(\sqrt{3} \times \sqrt{3})R30^\circ$ diffraction patterns on 6H-SiC(0001) surfaces prepared via exposure to 3000 sccm of hydrogen at $1500\ ^\circ\text{C}$ for 5 min. However, because of the need to investigate the efficacy of our cleaning procedures on the etched samples (see below) at elevated temperatures, the deposition of the heat absorbing tungsten coating and the *ex situ* cleaning step were employed as described in Sec. II. These procedures resulted in chemical changes to the surface and the occurrence of the (1×1) surface structure. The XPS spectra revealed silicon-carbon bonding, silicon-oxygen bonding, and adventitious hydrocarbons. The chemical composition of the silicon oxide layer was calculated to have a silicon-to-oxygen ratio of 1:4. An AES spectrum of the silicon-terminated surface of these samples shown in Fig. 4(a) had a calculated silicon-to-carbon ratio, uncorrected for sensitivity factors, of ~ 0.6 , as shown in Table III.

Annealing selected samples with hydrogen etched surfaces (see Table I) in UHV for 15 min at $1030\ ^\circ\text{C}$ reduced the oxygen level to concentrations below the detection limits of our AES instrument, as shown in Fig. 4(b). A $(\sqrt{3} \times \sqrt{3})R30^\circ$ reconstruction was obtained, as shown in Fig. 3(b). This annealing temperature was higher than the $930\ ^\circ\text{C}$

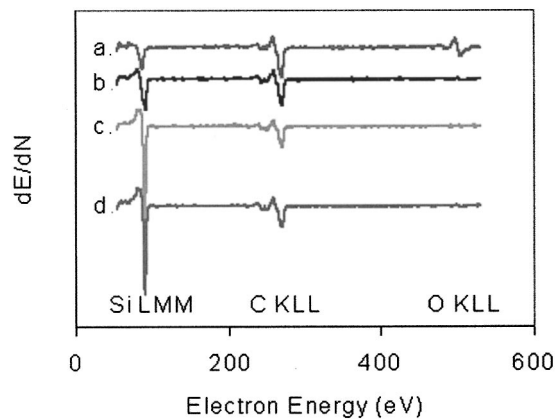


FIG. 4. AES survey spectra from a hydrogen etched 6H-SiC(0001) surface. (a) As-loaded, (b) $(\sqrt{3} \times \sqrt{3})R30^\circ$ reconstructed surface achieved via thermal annealing in UHV for 15 min, (c) 3×3 reconstructed surface achieved via a silane clean in 3000 L of SiH_4 at 1030°C for 10 min, and (d) a 1×1 surface achieved after annealing the 3×3 surface at 1030°C for 10 min.

950°C range necessary for the removal of the oxide from unetched samples. Annealing temperatures greater than 1000°C were also required for oxide removal in the AES and LEED studies conducted by Bernhardt *et al.*,⁵ who attributed the necessity of the higher temperatures to saturated surface bonds and shielding by a silicate layer.

The uncorrected silicon-to-carbon peak-to-peak height (pph) ratio in this research was calculated to be 1.2, as indicated for sample (b) in Table III. As would be expected, this value is lower than the reported value of 2.21 for 4H-SiC(0001) cleaned in a silicon flux,¹⁷ but higher than the ratio of ≤ 1.0 reported King *et al.*¹⁸ for unetched samples annealed under UHV at 1000°C . XPS of a similar sample, processed under the same etching, tungsten coating, and *ex situ* cleaning conditions except annealed in a gas source molecular beam epitaxy chamber using the same conditions

TABLE III. Peak positions and peak-to-peak height ratios for various hydrogen etched and cleaned surfaces of 6H-SiC(0001). Where applicable, these data are representative for samples with both values of $(N_D - N_A)$ shown in Table I.

Sample preparation LEED pattern	Silicon (LMM)		Carbon (KLL)		Si/C ratio
	position (eV)	Si_{p-p} height	Position (eV)	C_{p-p} height	
(a) Hydrogen etched; as loaded; (1×1)	87.5	316	270	523	0.6
(b) Hydrogen etched; annealed 1030°C –15 min in UHV; $(\sqrt{3} \times \sqrt{3})R30^\circ$	91.5	527	271	448	1.2
(c) Hydrogen etched; exposed to SiH_4 at 1030°C –10 min (CVC) (3×3)	90.5	1354	270.5	348	3.9
(d) CVC; annealed 1030°C for 10 min; (1×1)	90.5	1341	270	389	3.4

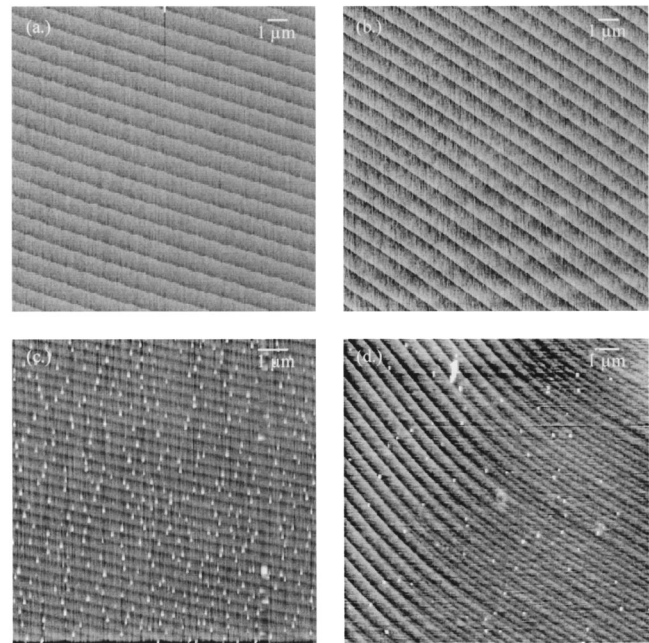


FIG. 5. AFM images from (a) as-loaded, (b) thermally annealed, (c) CVC cleaned, and (d) CVC cleaned and annealed hydrogen etched 6H-SiC(0001) surfaces. The white flecks are free silicon.

noted above confirmed the removal of the oxygen from the surface, the presence of a single carbon peak associated with the Si-C bond, and a nitrogen peak from residual ammonia. No evidence of graphite formation was observed. Figures 5(a) and 5(b) show AFM images of a sample before and after thermal desorption. The rms roughness of the surface did not change and was within $0.47 \text{ nm} \pm 0.01 \text{ nm}$.

The as-loaded, etched sample exposed to the CV clean using silane, showed a sharp (3×3) LEED pattern with a dark background, as shown in Fig. 3(c), indicative of an ordered surface. From the corresponding AES spectra, shown in Fig. 4(c), the uncorrected silicon-to-carbon pph ratio was calculated to be 3.9, as seen in Table III(c). This value is in the reported^{17,19} range of 3–5 for the 3×3 reconstruction observed on 6H-SiC(0001) and 4H-SiC(0001) surfaces. Exposure of the surface to silicon from the silane resulted in the deposition of silicon islands having a height ranging from 2.6 to 11.2 nm and a width of 50–100 nm that nucleated randomly across the surface, as shown in the AFM image in Fig. 5(c) rather than at particular locations on the steps. Fissel *et al.*²⁰ reported that for silicon quantum dots grown via molecular beam epitaxy on 6H-SiC(0001) at temperatures greater than 600°C , the transition to stress-induced Stranski-Krastanov growth of three-dimensional islands occurred before the deposition of a completed second monolayer of silicon. Kulakov *et al.*²¹ also noted that excess silicon deposited via evaporation at 850 – 1100°C on the (0001) surface of 6H-SiC surfaces during the formation of the (3×3) reconstruction resulted in the formation of islands.

Annealing the (3×3) 6H-SiC(0001) surface for an additional 10 min at 1030°C caused the LEED pattern to change to a 1×1 structure and the appearance of a diffuse ring, as

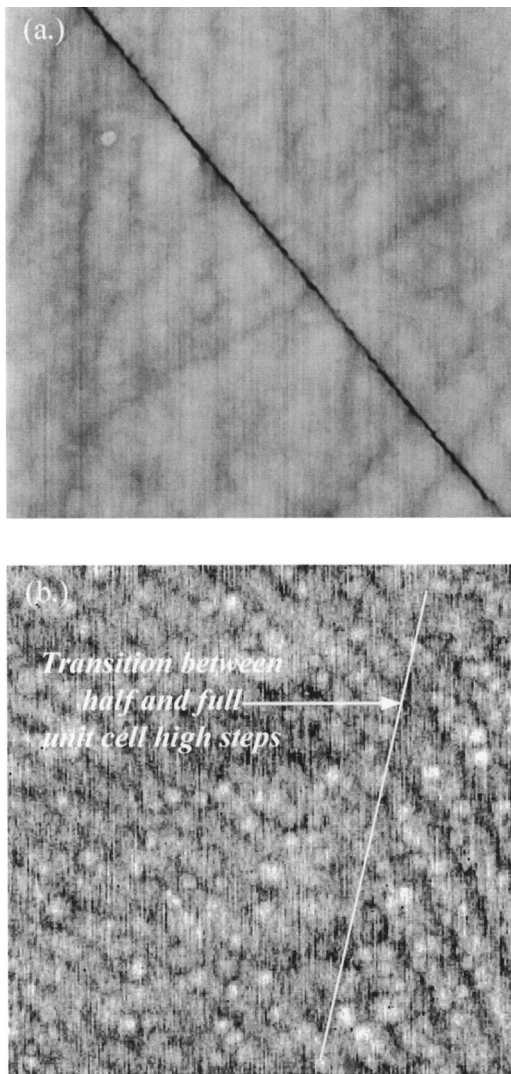


FIG. 6. (a) $10\text{ }\mu\text{m} \times 10\text{ }\mu\text{m}$ AFM scan of MOVPE grown AlN on an unetched 6H-SiC(0001). The rms roughness value is 1 nm; (b) $10\text{ }\mu\text{m} \times 10\text{ }\mu\text{m}$ AFM scan of MOVPE grown AlN on an etched 6H-SiC(0001) with $(N_D - N_A) = 8.7 \times 10^{17}\text{ cm}^{-3}$. The arrow indicates the transition region between unit cell high and one-half unit cell high steps on the surface. The rms roughness value is 0.4 nm.

shown in Fig. 4(d). The AES spectra, shown in Fig. 4(d) and summarized in Table III(d), showed an uncorrected Si/C pph ratio of 3.4 indicating some loss of silicon. The presence of residual silicon islands on the annealed surface was confirmed via AFM, as shown in Fig. 5(d). There was no effect of the height of the steps in the nucleation of the silicon islands.

C. AlN growth

The AlN films grown on both the unetched and the hydrogen etched wafers were without growth pits, as shown in the $10\text{ }\mu\text{m} \times 10\text{ }\mu\text{m}$ AFM scans in Figs. 6(a) and 6(b). The AlN on the unetched surface [Fig. 6(a)] reproduced the polishing scratches from the underlying substrate and had a surface rms roughness of ≈ 1.0 nm. The AlN on the hydrogen etched surface [Fig. 6(b)] reproduced the stepped structure of the

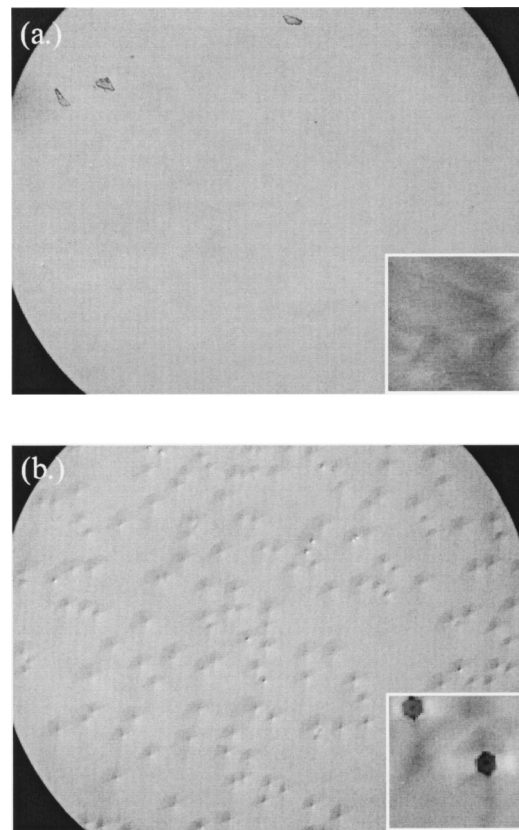


FIG. 7. (a) $200\times$ optical microscope images of MOVPE grown AlN on a hydrogen etched 6H-SiC(0001) substrate with $(N_D - N_A)$ of (a) $8.7 \times 10^{17}\text{ cm}^{-3}$; (b) $2.8 \times 10^{18}\text{ cm}^{-3}$. The inset in each figure shows a $35\text{ }\mu\text{m} \times 35\text{ }\mu\text{m}$ AFM image of the respective surface.

substrate, which, in the analyzed region, showed a transition between unit cell high and half unit cell high steps on a surface (see arrow). The rms roughness of this surface was ≈ 0.4 nm.

Optical micrographs of the surface microstructures at $200\times$ of the AlN films grown on hydrogen etched wafers containing the two different doping concentrations are shown in Figs. 7(a) and 7(b). The surface microstructures of these respective wafers were similar to those of analogous etched wafers shown in Figs. 1(a) and 1(b). When wafers with $(N_D - N_A) = 8.7 \times 10^{17}\text{ cm}^{-3}$ were used, the surface appeared smooth. The $40\text{ }\mu\text{m} \times 40\text{ }\mu\text{m}$ AFM image of the surface shown in the inset in Fig. 7(a) reveals facets with heights to 15 nm. The AlN film grown on the wafer with $(N_D - N_A) = 2.8 \times 10^{18}\text{ cm}^{-3}$ contained 120 nm deep hexagonal openings. The inset in Fig. 7(b) shows a $35\text{ }\mu\text{m} \times 35\text{ }\mu\text{m}$ AFM image of a portion of the surface containing two of the hexagonal pits. In essence, the microstructures of the SiC wafers were manifest in the AlN films. The films on both the etched and unetched surfaces were too resistive for electrical measurements.

IV. SUMMARY

Equilibrium thermodynamic calculations indicate that atomic hydrogen plays an important role in the decomposi-

tion of SiC and the formation of a hydrocarbon product in tandem with free Si and/or SiH₄. Atomic force and optical microscopy of the surfaces of 6H-SiC(0001) wafers with ($N_D - N_A$) of $2.5 \times 10^{18} \text{ cm}^{-3}$ etched in a flowing 25% H₂/75% He mixture at 1500 °C revealed a high density of screw dislocations with hexagonal unfilled cores (pits) relative to wafers with ($N_D - N_A$) of $7.5 \times 10^{17} \text{ cm}^{-3}$ etched at 1600 °C. Differences in the dislocation density were associated with the nitrogen concentration in the substrate. Atomic force microscopy of the etched surfaces of the latter sample showed regions with half unit cell height steps that may be indicative of surface regions of 3C-SiC stacking or stacking faults or both.

Cleaning the hydrogen etched (see Table I) surface via either thermal desorption of the native silicon oxide layer at 1030° for 15 min in UHV or exposure to a silicon flux (CV cleaned) had no effect on the step heights or their distribution produced during etching. AES analysis of the thermally desorbed wafers showed oxygen levels below the detection limit. LEED patterns of the thermally desorbed samples showed a strong ($\sqrt{3} \times \sqrt{3}$)R30° pattern, indicating a well-ordered surface structure. By contrast, cleaning with the silane flux produced a (3×3) LEED pattern, and the AES spectra showed an increase in the silicon-to-carbon ratio to 3.9. Atomic force microscopy revealed that the excess silicon had formed submicron islands at random points across the surface. Additional annealing produced a (1×1) LEED pattern and a diffuse ring. AES analysis indicated a slight drop in the amount of silicon; and AFM confirmed that islands were still present.

Films of AlN grown via MOVPE on etched and thermally desorbed 6H-SiC(0001) surfaces with ($N_D - N_A$) of $8.7 \times 10^{17} \text{ cm}^{-3}$ exhibited a rms roughness of $\approx 0.4 \text{ nm}$. The surface morphology of the AlN was improved when the films were grown on wafers with low net ionized impurity concentrations, as a result of the reduction in the number of hexagonal pits on the surface. The microstructure of the surface of the AlN films was a function of the concentration of hexagonal pits that were, in turn, a function of the density of screw dislocations. The latter appeared to be a function of the ($N_D - N_A$), but this hypothesis was not confirmed.

ACKNOWLEDGMENTS

This research was supported by the Department of Defense MURI Program via the Office of Naval Research under

Contract No. N00014-98-1-0654, J. Zolper, monitor and contract N00014-97-1-0859, Larry Cooper, monitor. The authors acknowledge V. Ramachandran and R. M. Feenstra of Carnegie Mellon University for selected samples, for useful discussion, and for assistance with the hydrogen etching. R. Davis was supported in part through Kobe Steel Ltd. Professorship. We gratefully acknowledge the support from Cree, Inc. who supplied the silicon carbide wafers used in this study.

- ¹B. N. Sverdlov, G. A. Martin, H. Morkoç, and D. J. Smith, *Appl. Phys. Lett.* **67**, 2063 (1995).
- ²V. M. Torres, J. L. Edwards, B. J. Wilkens, D. J. Smith, R. B. Doak, and I. S. T. Tsong, *Appl. Phys. Lett.* **74**, 985 (1999).
- ³F. Owman, C. Hallin, P. Mårtensson, and E. Janzen, *J. Cryst. Growth* **167**, 391 (1996).
- ⁴V. Ramachandran, M. F. Brady, A. R. Smith, R. M. Feenstra, and D. W. Greve, *J. Electron. Mater.* **27**, 308 (1998).
- ⁵J. Bernhardt, J. Schardt, U. Starke, and K. Heinz, *Appl. Phys. Lett.* **74**, 1084 (1999).
- ⁶Q. Xue, Q. K. Xue, Y. Hasegawa, I. S. T. Tsong, and T. Sakurai, *Appl. Phys. Lett.* **74**, 2468 (1999).
- ⁷T. L. Chu and R. B. Campbell, *J. Electrochem. Soc.* **112**, 955 (1965).
- ⁸M. Kumagawa and H. Kuwabara, *Jpn. J. Appl. Phys.* **8**, 421 (1969).
- ⁹C. Hallin, F. Owman, P. Mårtensson, A. Ellison, A. Konstantinov, O. Kordina, and E. Janzén, *J. Cryst. Growth* **181**, 241 (1997).
- ¹⁰A. A. Burk, Jr. and L. B. Rowland, *J. Cryst. Growth* **167**, 586 (1996).
- ¹¹A. Roine, *HSC Chemistry*, Version 2.03, Oktokumpu Research Oy, Pori Finland.
- ¹²N. Siebert, B. Mantel, Th. Seyller, J. Ristein, and L. Ley, *Diamond Relat. Mater.* **10**, 1291 (2001).
- ¹³A. Sagar, C. D. Lee, R. M. Feenstra, C. K. Inoki, and T. S. Kuan, *J. Appl. Phys.* **92**, 4070 (2002).
- ¹⁴J. M. Harris, H. C. Gatos, and A. F. Witt, *J. Electrochem. Soc.* **116**, 380 (1969).
- ¹⁵S. Nakamura, T. Kimoto, H. Matsunami, S. Tanaka, N. Teraguchi, and A. Suzuki, *Appl. Phys. Lett.* **76**, 3412 (2000).
- ¹⁶A. Okamoto, N. Sugiyama, T. Tani, and N. Kamiya, *Mater. Sci. Forum* **264-268**, 21 (1998).
- ¹⁷U. Starke, J. Schardt, and M. Franke, *Appl. Phys. A: Mater. Sci. Process.* **A65**, 587 (1997).
- ¹⁸S. W. King, R. S. Kern, M. C. Benjamin, J. P. Barnak, R. J. Nemanich, and R. F. Davis, *J. Electrochem. Soc.* **146**, 3448 (1999).
- ¹⁹R. Kaplan, *Surf. Sci.* **215**, 111 (1989).
- ²⁰A. Fissel, K. Pfennighaus, and W. Richter, *Appl. Phys. Lett.* **71**, 2981 (1997).
- ²¹M. A. Kulakov, G. Henn, and B. Bullemer, *Surf. Sci.* **346**, 49 (1996).